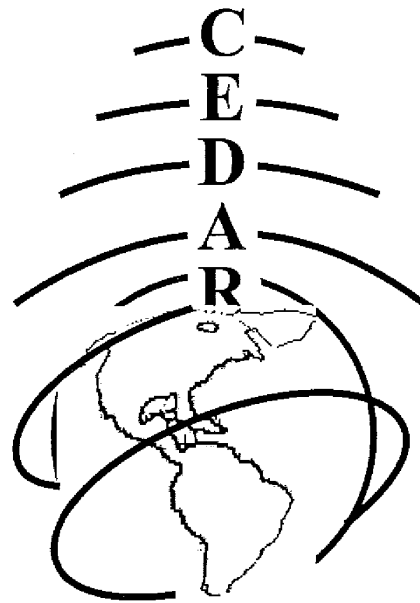




CEDAR-GEM Joint Workshop

Santa Fe, New Mexico

June 26 – July 1, 2011



CEDAR MLT Poster Session Booklet

Tuesday, June 28, 2011



Table of Contents

Instruments and Techniques for the Middle Atmosphere

ITMA-01 , Cody Vaudrin, University of Colorado Software Defined Multistatic Radar: System Development Update and Recent Results.....	1
ITMA-02 , Steve Watchorn, Spatial Heterodyne Spectroscopy to Determine [O] in the MLT Region	1

Meteor Science other than Wind Observations

METR-01 , Jongmin Choe, Anisotropy of the meteor decay times measured by a meteor VHF radar at King Sejong Station 62S, 57W), Antarctica	2
METR-02 , Elizabeth Bass, Simultaneous Meteor Observations Using High-Power, Large-Aperture and Specular Radars	2
METR-03 , Ryan Volz, Improving Radar Observation of Meteors using Compressed Sensing.....	3
METR-04 , Jeong-Han Kim, Mesospheric temperature estimation from the meteor decay times observed at southern high latitude.....	3
METR-05 , Alex McDonnell, Improved Meteor Deceleration and Mass Calculations Using Doppler Data from the ALTAIR HPLA Radar	3
METR-06 , Elizabeth Ann McCubbin, Classifying meteor trail echoes detected by the mid-latitude Super Dual Auroral Radar Network	4

Mesosphere and Lower Thermosphere Gravity Waves

MLTG-01 , Steve Smith, Gravity wave coupling between the mesosphere and thermosphere over New Zealand	4
MLTG-02 , Thomas Boyd Martin, Comparison of Long-period to Short-Period Gravity Waves Over Petrolina, Brazil and Halley, Antarctica.....	4
MLTG-03 , Fabio Vargas, Evidence of the influence of high frequency gravity waves on the meridional residual circulation.....	5
MLTG-04 , Fabio Vargas, Gravity wave parameter estimation using collocated airglow, wind and temperature data recorded at 23°S.....	5
MLTG-05 , Uday Kanwar, Estimation of the Vertical Wavelength of Atmospheric Gravity Waves from Airglow Imagery	5
MLTG-06 , Edward Grabenhorst, Infrared Measurements of Hydroxyl Airglow Emissions and Gravity Wave Perturbations over Daytona Beach, Florida.....	5
MLTG-07 , Zhenhua Li, An Investigation on Gravity Wave Characteristics Observed by Airglow Imager at Maui, HI	6
MLTG-08 , Richard George, The Effects of Gravity Waves On Airglow and Minor Species in The MLT Region.....	6
MLTG-09 , Changsup Lee, Seasonal variations of the gravity wave activity in the mesopause region at King Sejong Station (62.22°S, 58.78°W), Antarctica.....	7
MLTG-10 , Igo Paulina, Forward ray-tracing of medium-scale gravity waves in the MLT region over Brazil	7
MLTG-11 , Jonathan Pugmire, Mesospheric Temperature Variability Over The Andes Mountains.....	7
MLTG-12 , Neal Criddle, Seasonal Variability and Dynamics of Mesospheric Gravity Waves Over the Andes Mountains	8
MLTG-13 , Kim Nielsen, Airglow Imaging of Polar Atmospheric Gravity Waves over Poker Flat, Alaska	8
MLTG-14 , Kim Nielsen, Fourier Ray Tracing of Atmospheric Gravity Waves Utilizing a Numerical Weather Prediction System.....	8
MLTG-15 , Xian Lu, Comparative studies on the tidal modulations of the GW variances in the MLT region using the meteor radar	9
MLTG-16 , Laura Holt, Gravity waves in WACCM with respect to transport of NO _x created by energetic particle precipitation.....	9
MLTG-17 , Chihoko Yamashita, Physical Mechanisms of Gravity Wave Variations and Their Impacts on the MLT during the 2009 Stratospheric Sudden Warming	10

Mesosphere and Lower Thermosphere Lidar Studies

MLTL-01 , Xinzhao Chu, First Results from McMurdo Lidar Campaign	10
MLTL-02 , Weichun Fong, Temperature Profiling from McMurdo, Antarctica with a Fe	11
MLTL-03 , Cao Chen, Wave signatures in Fe temperature measurements over McMurdo	11
MLTL-04 , Wentao Huang, Simultaneous and Common-Volume Lidar Observations of Mesospheric Na and Fe Layers at Boulder, Colorado (40N, 105W) in 2010	11
MLTL-05 , Richard Collins, Lidar Studies of the Arctic Atmosphere at Chatanika, Alaska	12
MLTL-06 , Britta Irving, Mesospheric inversion layers seen by Rayleigh lidar and their relationship to planetary wave structure in the Arctic middle atmosphere	12
MLTL-07 , Leda Sox, The World's Most Sensitive Rayleigh-Scatter Lidar	13
MLTL-08 , Tony Mangogna, Resonance Fluorescence He LIDAR	13
MLTL-09 , Robert Andrew Stillwell, Accounting for nonlinear sensor behavior in laser remote sensing applications	13

Mesosphere or Lower Thermosphere General Studies

MLTS-01 , Rachel Ward, With My Head in the Clouds: Helping to Understand the Boundary Between Earth and Space	14
MLTS-02 , Justin Carstens, Analysis of the PMC Parameter Retrieval from a CIPS Scattering Profile: High Sensitivity to Uncertainties and Methods Used to Account for this	14
MLTS-03 , Brentha Thurairajah, AIM/CIPS observation and NOGAPS-ALPHA analysis of polar mesospheric cloud structures	15
MLTS-04 , Cissi Ying-tsen Lin, Solar Energy and Nitric Oxide in the Lower Thermosphere: Observations by the Remote Atmospheric Ionospheric Detection System (RAIDS) and the Solar Dynamic Observatory (SDO)	15
MLTS-05 , Karthik Venkataramani, Simulating Nitric Oxide in the lower Thermosphere using a 3D model	16
MLTS-06 , Justin Yonker, The Role of N ₂ (A) in Production of Lower Thermospheric Nitric Oxide (NO)	16
MLTS-07 , Bo Tan, Tele connection pattern of different altitudes and different hemispheres derived from SABER and WACCM	16
MLTS-08 , Martin Langowski, Investigation of metal and metal ion density profiles in the MLT by satellite remote sensing using data from SCIAMACHY	17
MLTS-09 , Deepali Vimal Saran, Iron Oxide Emission in the Mesosphere	17
MLTS-10 , Deepali Vimal Saran, Relaxation of O ₂ (v = 1) by Atomic Oxygen and Carbon Dioxide	18
MLTS-11 , Jerome Thiebaud, Vibrational Relaxation of OH(v = 7) with O, O ₂ , and N ₂ , presented by Konstantinos Kalogerakis	18
MLTS-12 , Victor Pasko, Finite-difference time-domain modeling of infrasonic waves generated by supersonic auroral arcs	19
MLTS-13 , Kishore Kumar Grandhi, Simultaneous observations of meteor echoes with different frequencies (32.55 MHz and 53.5 MHz)	20
MLTS-14 , Wayne Hocking, Long term behaviour of the MLT quasi-7-day wave at two radar-sites at northern polar latitudes, presented by Kishore Kumar Grandhi	20
MLTS-15 , Fontenla Juan, Solar Spectral Irradiance effects on the heating and chemistry of the stratosphere and mesosphere	21
MLTS-16 , Chad Fish, Long-term Observations of Winds and Waves over Bear Lake Observatory	21

Mesosphere and Lower Thermosphere Other Tidal or Planetary Waves

MLTT-01 , Ana Roberta Paulina, A possible effect of the 2006 Sudden Stratospheric Warming in the lunar semidiurnal tide	21
MLTT-02 , Irfan Azeem, Dynamical Response in the Mesosphere and Lower Thermosphere to a Sudden Stratospheric Warming Event in the Southern Hemisphere During 2010	22

MLTT-03 , Frederico Estante, Short-term variability of the $s=1$ nonmigrating semidiurnal tide over the South Pole due to coupling with Northern Hemisphere wave activity	22
MLTT-04 , Jia Yue, Quasi-two-day waves in the lower thermosphere.....	22
MLTT-05 , Gong Yun, Incoherent scatter radar study of the terdiurnal tide in the E- and F-region heights at Arecibo	23
MLTT-06 , Katelynn Greer, Planetary Wave Disturbances of the Wintertime Polar Upper Stratosphere and Lower Mesosphere: A Summary of Observed Characteristics	23

Sprites

SPRT-01 , Burcu Kosar, Sprite Streamer Formation in Under-Voltage Conditions.....	24
SPRT-02 , Samaneh Sadighi, Streamer Discharges From Isolated Hydrometeors in Thunderclouds.....	24
SPRT-03 , Jianqi Qin, Impact of mesospheric ion conductivity variations on the initiation of long-delayed sprites.....	25
SPRT-04 , Caitano Luiz da Silva, Influence of the charge moment change on sprite initiation altitude.....	25
SPRT-05 , Wei Xu, Monte Carlo Simulation of Terrestrial Gamma-ray Flashes.....	25
SPRT-06 , Sotirios Mallios, Charge transfer to the ionosphere and to the ground during thunderstorms.....	26

Stratosphere Studies and Below

STRB-01 , Aman Chandran, An analysis of SSW & elevated stratopauses generated in WACCM	26
STRB-02 , Chao-Hsin Chen, An Investigation of Gamma Drop Size Distribution aloft using the Chung-Li VHF Radar	27

Global Positioning System

IT-GPS-01 , Justin Gyllen, Possibilities for Calibrating GPS TEC with ISR Data	27
---	----

CEDAR GEM Joint Workshop – MLT Poster Session Abstracts Day 1 – Tuesday, June 28, 2011

Instruments and Techniques for the Middle Atmosphere

ITMA-01 University of Colorado Software Defined Multistatic Radar: System Development Update and Recent Results - by Cody Vaudrin

Status of First Author: Student IN poster competition

Authors: Cody Vaudrin, Scott Palo

Abstract: The Colorado Software Defined Radar (CoSRad) is presented as a data acquisition and radar control system. Using a software configurable common hardware platform, the system is capable of integration with a wide range of existing radar systems and can serve as the control and data acquisition hardware for new radar systems. Based on the software defined radio model, CoSRad enjoys a number of performance enhancements over comparable fixed-frequency analog systems. System performance is quantified using various metrics based on of sampling, sample rate conversion, data processing capabilities, SNR and networkability. Gains in SNR are made by decreasing the number of discrete components involved in RF analog processing, oversampling the band-limited return signal and encoding the return using a 14-bit ADC. Most important to the field of geophysical remote sensing radar is CoSRad's rapid software-based reconfigurability and comparatively low cost. CoSRad has been successfully integrated with a number of radar systems including SAMMER, Cobra and the NOAA W-band profiler with plans for integration with JRO's JASMET radar in the near future. Furthermore, GPS-based synchronization of multiple CoSRad receivers enables multistatic radar measurements. Finally, a plan for a multistatic meteor trail measurement is outlined.

ITMA-02 Spatial Heterodyne Spectroscopy to Determine [O] in the MLT Region - by Steve Watchorn

Status of First Author: Non-student

Authors: Steve Watchorn (steve@sci-sol.com) and John Noto of Scientific Solutions

Abstract: As the dominant neutral species between 250 and 500 km altitude (Lancaster [1997]), neutral oxygen plays a vital role in the physics of the thermosphere. It transports energy downward from the thermosphere via O₂ photolysis [Thomas, 1990], and is important in many airglow production processes, including O₂, OI, and OH [Chamberlain, 1961]. Despite its great importance, measurements of the density of the neutral oxygen, [O], are not extensive. Since the end of the 1970s, the heyday of the Dynamics Explorer, there has been a lack of comprehensive mass spectrometer data needed to investigate [O]. Measurements since then have been primarily drawn from rocket- and satellite-based observations, which have poor local time coverage [Harrell, et. al., 2010], and are also expensive and relatively risky. Previous ground-based methods for making the determination using concerted OI (557.7 nm), atmospheric O₂, and OH Meinel airglow measurements, which requires an initial assumption of the layer shape. A more direct method for determining [O] comes from recent examinations of the intensity ratio of the D2 to D1 lines of the sodium doublet near 589 nm. Following the discussion in [Slanger, et. al., 2005], the sodium emission from the Earth's atmosphere is due to the transition (3²PJ - 3²S1/2), from a layer at approximately 90 - 100 km, near the turbopause at the lower edge of the thermosphere. The emission was postulated by Chapman to result from a sequence of reactions showing the interaction of sodium with oxygen.

The success of this project will make possible the installation of similar instruments at many sites around the world, for broader coverage of [O] measurements to improve global models of the mesosphere and lower thermosphere. Previous measurements have been wed to large telescopes like Keck I and II,

necessitating long exposures and limiting observation locations and times. The spatial heterodyne spectrometer (SHS) proposed for this project will be dedicated to sodium nightglow observations (unlike a larger, bulkier spectrometer like CESAR) as a stand-alone instrument with limited power, space, and environmental control requirements. Developing such instruments for Na observations, and other observations in the visible -- and making them available to multiple sites around the world, will be a boon to global aeronomy.

In addition, this project fosters collaboration between small business (Scientific Solutions, Inc.) and university research institutions (Purple Crow / University of Western Ontario). A major part of the collaboration would be the involvement of a UWO student (either undergraduate or graduate; either can make suitable contributions) to the running of the SHS instrument upon its installation at Purple Crow in late Year One - early Year Two of the project.

Meteor Science other than Wind Observations

METR-01 Anisotropy of the meteor decay times measured by a meteor VHF radar at King Sejong Station (62S, 57W), Antarctica - by Jongmin Choe

Status of First Author: Student IN poster competition, Undergraduate

Authors: Jongmin Choe(a), Yong Ha Kim(a), Changsup Lee(a), Jeong-Han Kim(b), and Geonhwa Jee(b)
(a)Department of Astronomy and Space Science, Chungnam National University, Daejeon, Korea
(b)Korea Polar Research Institute, Incheon, Korea

Abstract: We have analyzed meteor decay times measured by a VHF meteor radar at King Sejong Station, Antarctica to study diffusion processes of the meteor trails near the mesopause region. Since the installation of the radar in 2007, it has been recorded decay times of about 20,000 meteors a day over all sky at the height of 70 to 110 km. Above the altitude of 93 km, diffusion of ions in a meteor trail can be greatly affected by the existence of geomagnetic field, which may cause the distribution of measured decay times to be anisotropic over the azimuthal and elevation angles. Our preliminary analysis seems to confirm the anisotropic nature of meteor decay times above about 93 km altitude, which is consistent with a study by Hocking (2005). Height profiles of the measured meteor diffusion coefficients were compared with the theoretical profiles from Elford & Elford (1999), which shows remarkable similarity above about 93 km altitude.

METR-02 Simultaneous Meteor Observations Using High-Power, Large-Aperture and Specular Radars - by Elizabeth Bass

Status of First Author: Student IN poster competition, PhD

Authors: Elizabeth Bass (enb@bu.edu), Boston University; Meers Oppenheim, Boston University; Jorge Chau, Jicamarca Radio Observatory

Abstract: For over six decades, specular meteor radars have measured properties of the meteoroid population and inferred wind speeds in the Mesosphere and lower Thermosphere (MLT). High-power, large-aperture (HPLA) radars have been utilized more recently for similar studies. Despite the extensive use of these instruments, there is a lack of simultaneous observations with both systems that would allow a direct comparison of their measurements. In September 2009, concurrent observations were conducted using the 50 MHz incoherent scatter radar at the Jicamarca Radio Observatory (JRO) in Peru and a meteor radar system located approximately 200 km away in Paracas. In this poster, we compare the signals received from meteors detected with both radars, verified by signal timing and meteoroid trajectory, estimate meteoroid sizes and infer wind speeds.

METR-03 Improving Radar Observation of Meteors using Compressed Sensing
by Ryan Volz

Status of First Author: Student IN poster competition, PhD

Authors: Ryan Volz, Stanford University, Department of Aeronautics and Astronautics, rvolz@stanford.edu; Sigrid Close, Stanford University, Department of Aeronautics and Astronautics, sigridc@stanford.edu

Abstract: Current meteor observation techniques using high-power large-aperture (HPLA) radars often overlook the complexities of scattering from a distributed plasma target, leading to difficulties in confidently interpreting the results. We demonstrate a measurement approach based on compressed sensing that is suitable for distributed targets and allows improved range resolution, complete noise filtering, and identification of multiple Doppler shifts within the same range window. Through comparisons with matched filter processing, we show that our compressed sensing technique gives valid results with the potential to provide new insights into meteor plasma physics.

METR-04 Mesospheric temperature estimation from the meteor decay times
observed at southern high latitude - by Jeong-Han Kim

Status of First Author: Non-student

Authors: Jeong-Han Kim¹, Yongha Kim², and Geonhwa Jee¹
¹Korea Polar Research Institute, Incheon, Korea
²Chungnam National University, Daejeon, Korea

Abstract: We have been operated a VHF meteor radar at King Sejong Station (62.2°S, 58.8°W), Antarctica since March 2007 for the observations of the neutral winds in the mesosphere and lower thermosphere region. The radar observation also allows us to estimate the neutral temperature from the measured meteor decay times of the meteor echoes by utilizing a method presented by Hocking (1999). For this temperature estimation, the meteor echoes observed from March 2007 to October 2009 were divided into weak and strong echoes depending on the strength of estimated relative electron line densities, whereas previous studies have used all echoes without classification by echo strength. In this study, we discuss the slope determination of log inverse decay time vs. height graph, which is used in temperature estimation and present the estimated temperatures for each group. We also compare the estimated temperatures with the temperature measurements from the spectral airglow temperature imager (SATI), which has also been operated at the same location since 2002, and the SABER instrument onboard TIMED satellite.

METR-05 Improved Meteor Deceleration and Mass Calculations Using Doppler
Data from the ALTAIR HPLA Radar - by Alex Macdonell

Status of First Author: Student IN poster competition, Masters

Authors: Alex Macdonell, Boston University, amacdne@bu.edu; Rohan Loveland, Los Alamos National Laboratory, roloveland@lanl.gov; Meers Oppenheim, Boston University, meerso@bu.edu; Sigrid Close, Stanford University, sigridc@stanford.edu; Elizabeth Bass, Boston University; Patrick Colestock, Los Alamos National Laboratory

Abstract: High Power Large Aperture (HPLA) radars, such as ALTAIR, Jicamarca, and Arecibo, have been used extensively to study meteoroid populations for the last decade, but fundamental questions still remain about how to best analyze and interpret the data. This poster presents results from a new method of evaluating meteor velocities, using Doppler data from the ALTAIR HPLA radar. To overcome Doppler aliasing problems, this method applies an approximation of quadratic integer programming to unwrap the phase differences observed in the radar's matched filter time response, based on an underlying assumption of smoothness in the meteor deceleration profile. This results in a family of solutions which can be

disambiguated using a simple range-differencing calculation. The true 3-D velocities of the meteors can then be extracted by utilizing in-beam positioning information provided by ALTAIR's monopulse system. Results are given for a large set of meteor head echoes taken from a data collect conducted with ALTAIR in 2007, and include velocity, deceleration, and dynamical mass distributions. Lastly, this poster presents comparisons between the deceleration and scattering masses.

METR-06 Classifying meteor trail echoes detected by the mid-latitude Super Dual Auroral Radar Network - by Elizabeth Ann McCubbin

Status of First Author: Student IN poster competition, PhD

Authors: Elizabeth A. McCubbin; Simon G. Shepherd

Abstract: Dartmouth College led the build of two coherent backscatter radars with 24 beams near Christmas Valley, Oregon in November as part of the collaboration to develop a network of mid-latitude radars know as the Super Dual Auroral Radar Network (SuperDARN). Currently research on near-range backscattering drifts are analyzed on determining the classification of meteors trail echoes from other backscattering echoes such as E-region irregularities and background noise occurring at mid-latitudes. With two radars in close proximity, a comparison on derived velocities show different results that may be caused from E-region plasma drifts that have similar characteristics of meteor trail echoes. A clear distinguish on classifying meteor trail echoes can be used to develop a global analysis of neutral winds with multiple SuperDARN radars around the mid-latitude region.

Mesosphere and Lower Thermosphere Gravity Waves

MLTG-01 Gravity wave coupling between the mesosphere and thermosphere over New Zealand - by Steve Smith

Status of First Author: Non-student

Authors: Steve Smith, Gonzalo Hernandez, W. Jack Baggaley and Jeffrey Baumgardner.

Abstract: Direct evidence of dynamic coupling between the mesosphere and thermosphere at mid-latitudes is presented. During a large breaking gravity wave event in the upper mesosphere, an unusual pair of gravity wave events was observed in all-sky images of the thermospheric atomic oxygen O(1D) 630.0 nm emission. The images were obtained with the Boston University all-sky imaging system located at the Mount John Observatory, New Zealand (43.98°S, 170.42°E).

MLTG-02 Comparison of Long-period to Short-Period Gravity Waves Over Petrolina, Brazil and Halley, Antarctica - by Thomas Boyd Martin

Status of First Author: Student IN poster competition, Undergraduate

Authors: T. Martin, M. J. Taylor, D. Pautet, M. J. Jarvis

Abstract: Previous analysis has been done for short-period gravity waves all around the globe. The Center for Atmospheric Space Science department at USU has all-sky imagers in Petrolina (9°S), Brazil and Halley (76°S), Antarctica, to capture images of air-glow OH emission levels (~87km). With a newly developed method, keograms are produced for analysis of larger-scale gravity waves. Characteristics of long and short-period gravity waves at the same latitude are compared. Strong similarities are observed in the wave directionality. Parameters, such as horizontal wavelength and wavespeed, and the observed period, have been measured in high-latitude and equatorial regions, and show strong similarities for long-period gravity waves' characteristics. Further analysis will be done over these regions to develop a climatology of long-period gravity waves.

MLTG-03 Evidence of the influence of high frequency gravity waves on the meridional residual circulation - by Fabio Vargas

Status of First Author: Non-student

Authors: Fabio Vargas, UIUC, fvargas@illinois.edu; Gary Swenson, UIUC, swenson1@illinois.edu

Abstract: The meridional residual circulation in the MLT region is the result of the thermal adjustment of the atmosphere due to the forcing imposed by dissipating atmospheric gravity waves (AGW) on the zonal wind. This work will show evidences of a meridional stress likely imposed by high frequency AGWs on the residual circulation, a quantitative estimation of its forcing measured through the momentum flux divergence of AGWs observed in multilayer airglow images and a discussion of the impact that it could have on the predictions of global circulation models.

MLTG-04 Gravity wave parameter estimation using collocated airglow, wind and temperature data recorded at 23°S - by Fabio Vargas

Status of First Author: Non-student

Authors: Fabio Vargas, UIUC, fvargas@illinois.edu; Gary Swenson, UIUC; Paulo Batista, INPE; Delano Gobbi, INPE; Barclay Clemesha, INPE; Dale Simonich, INPE

Abstract: A multicolor imager, Na lidar and meteor radar were operated in Brazil at 23° S during 2007-2008 giving 21 days of coincident airglow image, temperature and wind measurements. The present dataset allowed to estimate intrinsic parameters of gravity waves observed in airglow images considering a variable static stability and a sheared atmosphere. Multilayer observation permitted to calculate the wave momentum flux and flux divergence in a realistic manner and study the vertical propagation of gravity waves under variable atmospheric fields, which in turn generates critical levels, instable regions and ducting (Thermal/Doppler) in the MLT.

MLTG-05 Estimation of the Vertical Wavelength of Atmospheric Gravity Waves from Airglow Imagery - by Uday Kanwar

Status of First Author: Student IN poster competition, Masters

Author: Uday Kanwar

Abstract: Atmospheric gravity waves (AGWs) are associated with energy and momentum transfer from the troposphere to the mesosphere and lower thermosphere. They are known to affect the chemistry of the ozone and climate as well as alter large-scale winds and temperatures. In order to be able to quantify these effects it is imperative to determine their wave parameters. A non-tomographic technique [Anderson 2009] to estimate the parameters of AGWs is augmented using airglow data at three different heights recorded by two ground-based imaging systems located in New Mexico. The magnitude and phase of an airglow perturbation model are analyzed independently to arrive at estimates for the vertical wavelength. Results are then presented and it is shown that the estimates using the phase and magnitude compare well.

MLTG-06 Infrared Measurements of Hydroxyl Airglow Emissions and Gravity Wave Perturbations over Daytona Beach, Florida - by Edward Grabenhorst

Status of First Author: Student IN poster competition, Undergraduate

Authors: Ali, Christopher; Heale, Christopher; Snively, Jonathan; Sivjee, Abas; Hickey, Michael; Liu, Alan

Abstract: Optical observations of gravity waves, propagating in the mesosphere and lower-thermosphere (MLT) region of Earth's atmosphere, are now routinely obtained via imaging their perturbations to hydroxyl (OH Meinel band) airglow emissions occurring at ~ 87 km altitude [e.g., Taylor et al., JGR, 102, 26283, 1997; Walterscheid et al., JASTP, 61, 461, 1999]. Embry-Riddle Aeronautical University currently houses instruments which measure OH emission spectra from 1000-2000nm, allowing determination of OH intensity and rotational temperature. To complement these data, an infrared camera capable of high time resolution measurements is being configured to capture spatial and temporal variations of the OH(2-0), OH(3-1) and OH(4-2) band emissions as a result of gravity waves [e.g., Taylor et al., COSPAR, 2011]. Resolving these additional data will allow determination of wavelength and direction of propagation. The high temporal resolution of the instrument will allow fast wave processes such as breaking to be clearly resolved. The dominant gravity wave sources in Daytona Beach, Florida are expected to be associated with convective activity, as no local mountain wave sources exist, thus providing insight into weather-related gravity wave forcing. In this poster we present details of the instrument design and capabilities, and investigate the expected local gravity wave sources and seasonal variations of viewing conditions.

MLTG-07 An Investigation on Gravity Wave Characteristics Observed by Airglow Imager at Maui, HI - by Zhenhua Li

Status of First Author: Student NOT in poster competition

Authors: Zhenhua Li, Alan Liu, Xian Lu , Gary Swenson

Abstract: Gravity wave occurrence frequency and propagation direction observed in the mesopause region over Maui, HI shows clear seasonal change. This seasonal change is caused by convective source variation and background atmospheric condition changes. Wave transmission through the lower atmosphere and ducting condition in the mesopause, lower thermosphere region are two major factors causing the observed seasonal variation in wave occurrence frequency.

MLTG-08 The Effects Of Gravity Waves On Airglow And Minor Species in The MLT Region - by Richard George

Status of First Author: Student IN poster competition, Undergraduate

Authors: Richard George and Tai-Yin Huang; Physics Department, Penn State Lehigh Valley, Center Valley, PA, USA.

Abstract: Gravity wave effects on airglow in the Mesosphere and Lower Thermosphere (MLT) region are investigated by using a 2-D OH and Multiple Airglow Chemistry Dynamics (MACD) model, both of which include a spectral full wave model and a chemistry model. The 2-D OH model includes the OH nightglow chemistry and the MACD includes the greenline and O₂ atmospheric band nightglow chemistry. The spectral full wave model simulates a propagating, dissipating gravity wave packet with a forcing wave period of 20 minutes and a horizontal wavelength of 30 km at 18 degrees north. Wave-induced variations of minor species and the three airglow emissions will be simulated and analyzed; the three airglow emissions being investigated are OH(8,3), O₁S (greenline), and O₂(0,1) atmospheric band. Specifically what is being investigated are the gravity-wave packet's effect on the minor species and airglow intensity variations, secular variations, and fluctuations. Our study shows that airglow intensity variations of OH(8,3), O₁S, and the O₂(0,1) atmospheric band increase by 25%, 33%, and 30%, respectively, by the end of the simulation time. We will do further analysis to deduce the wave-induced airglow intensity variations.

MLTG-09 Seasonal variations of the gravity wave activity in the mesopause region at King Sejong Station (62.22°S, 58.78°W), Antarctica
by Changsup Lee

Status of First Author: Student IN poster competition, PhD

Authors: Changsup Lee 1, Yong Ha Kim 1, Jongmin Choe 1, Jeong-Han Kim 2, Geonhwa Jee 2
1 Department of Astronomy and Space Science, Chungnam National University, Daejeon, Korea
2 Korea Polar Research Institute, Incheon, Korea

Abstract: We calculated wind variances from the horizontal wind data obtained from the meteor radar measurements at King Sejong Station (KSS), Antarctica. The wind variances can be used to obtain parameters for wave activities in the mesopause region. The least square method using radial velocity directly measured and the radial component composed of hourly mean horizontal winds (zonal, meridional directions) has been used to estimate horizontal wind variance across 80-100 km height region. Although the seasonal and height dependence of the horizontal wind variances are in agreement with those from the measurements at Rothera station (67.57°S, 68.13°W) not far from KSS, the magnitude becomes 2 or 3 times greater than the values at Rothera, which may indicate that the gravity waves are more active at KSS than at Rothera due to the topographical structures around the KSS. The location of KSS is near the tip of the Antarctic peninsula, where the gravity wave activity in the troposphere has been reported to be strong. In order to validate the strong gravity wave activity, we will compare our wind variances with temperature variances measured by SABER over KSS in the same period.

MLTG-10 Forward ray-tracing of medium-scale gravity waves in the MLT region over Brazil - by Igo Paulino

Status of First Author: Student NOT in poster competition

Authors: I. Paulino (INPE, Brazil); H. Takahashi (INPE, Brazil); S. L. Vadas (CoRA, USA); C. M. Wrasse (VSE, Brazil); R. A. Buriti (UFCEG, Brazil); A. F. Medeiros (UFCEG, Brazil); D. Gobbi (INPE, Brazil); J. J. Makela (University of Illinois, USA); J. W. Meriwether (Clemson University, USA)

Abstract: Second SpreadFEx campaign was carried out from September to November 2009 in the Brazilian equatorial region. During the campaign, we observed 26 medium-scale gravity waves in the OHNIR airglow images and simultaneous plasma bubble occurrences. In the present work, we ray traced these waves in order to study their propagation conditions in the thermosphere-ionosphere. Thermospheric winds observed by a Fabry-Perot Interferometer and mesospheric winds by a meteor radar were used in the model calculation. Preliminary results reveal that some waves could propagate to high altitudes in the thermosphere-ionosphere region. Salient features will be discussed.

MLTG-11 Mesospheric Temperature Variability Over The Andes Mountains
by Jonathan Pugmire

Status of First Author: Student IN poster competition, PhD

Authors: J. R. Pugmire, M. J. Taylor, Y. Zhao, Center for Atmospheric and Space Sciences, Utah State University

Abstract: The Utah State University CEDAR Mesospheric Temperature Mapper (MTM) is a high-quality CCD imager capable of remote sensing faint optical emissions from the night sky to determine mesospheric temperature and its variability at an altitude of ~87 km. The MTM has operated continually at the new Andes Lidar Observatory (ALO) located at Cerro Pachon, Chile (30.2° S, 70.7° W) since August 2009 to investigate the seasonal characteristic of the mesopause at mid-latitudes. Measurement were made alongside a powerful lidar capable of height sounding the mesosphere. In this study, the MTM data have

been analyzed to determine night to night variability and seasonal characteristics in the OH band intensity and temperature induced by acoustic-gravity waves.

MLTG-12 Seasonal Variability and Dynamics of Mesospheric Gravity Waves Over the Andes Mountains - by Neal Criddle

Status of First Author: Student IN poster competition, Undergraduate

Author: Neal Criddle

Abstract: The ALO is a new facility developed for atmospheric research, located at the foot of the Andes mountain range in Cerro Pachon, Chile (30.2°S, 70.7°W). As part of a collaborative program, Utah State has a mesospheric temperature mapper (MTM) on site, which is used to study short period gravity wave dynamics and temperature variations in the mesosphere-lower thermosphere region. The MTM began taking measurements of the OH(6,2) and O₂(0,1) spectral bands in August 2009 and a complete profile of seasonal variation in gravity wave characteristics has been created for August 2009 through August 2010 using the OH(6,2) Band. The primary goal of this program is to:

- Quantify seasonal variability of gravity wave structures.
- Compare and contrast seasonal directionality and characteristic variability with results from the Maui-MALT oceanic site.
- Quantify mountain wave observations, their frequency, images, characteristics and seasonal variability.

Seasonal variability for gravity wave structures at this site is shown. Mountain waves have been exclusively observed to appear in the winter months. Future work includes verifying yearly repeatability, which is seen at other sites, and continued investigation of unique events occurring over the Andes mountain range.

MLTG-13 Airglow Imaging of Polar Atmospheric Gravity Waves over Poker Flat, Alaska - by Kim Nielsen

Status of First Author: Non-student

Authors: Kim Nielsen, Michael Taylor, Richard Collins

Abstract: A newly acquired airglow imager was installed at Poker Flat Research Range (PFRR) in January 2011 as part of a three year collaborative study between Computational Physics, Inc, University of Alaska, Fairbanks, and Utah State University. The main goals during this period are to establish a climatology regarding short-period gravity waves observed during the long winter months over an Arctic site. The location of PFRR is ideally situated for a study regarding the impact of sudden stratospheric warming events on these waves and the mesosphere in general. Furthermore, PFRR is located near large mountain ranges and in an area experiencing distinct weather systems, which translates into a broad range of potential wave sources and propagation conditions for the waves. In this presentation we will present initial results obtained during the first three months of operation.

MLTG-14 Fourier Ray Tracing of Atmospheric Gravity Waves Utilizing a Numerical Weather Prediction System - by Kim Nielsen

Status of First Author: Non-student

Authors: Kim Nielsen, David Broutman, David Siskind, Karl Hoppel, Michael Taylor

Abstract: Since the austral winter of 2000, Utah state University, in collaboration with British Antarctic survey, has operated an airglow imager at Halley and Rothera on the Antarctic continent. Climatological studies have shown the majority of the observed waves to exhibit freely propagating characteristics in the airglow region, suggestion these waves were generated in close proximity to their observation site, despite

the lack of any clear wave source. In this study, we utilize a Fourier ray tracing technique combined with wind and temperature data from a Numeric Weather Prediction (NWP) system, the Navy Operational Global Atmospheric Prediction System Advanced Level Physics and High Altitude (NOGAPS-ALPHA) to further improve our understanding of the origin of these waves.

MLTG-15 Comparative Studies on the tidal modulations of the GW variances in the MLT region using the meteor radar - by Xian Lu

Status of First Author: Student IN poster competition, PhD

Authors: Alan Z. Liu (ERAU); Steven J. Franke (UIUC)

Abstract: The diurnal and semidiurnal oscillations of the GW variances at three different locations are observed using the meteor radar. The GW variances are calculated based on the variances of the horizontal winds after subtracting the effects from mean winds, planetary waves, tides, longer-period GWs and high-frequency turbulences. The wave periods which can be efficiently resolved by this method are between 6 mins and 4 hrs. The horizontal scale is less than 500 km, which corresponds to the collecting volume of the meteor radar. A Monte-Carlo simulation is performed in order to find out the sensitivity of the GW variance calculation on the meteor rate. Two experiments about adding a single-GW and a GW spectrum onto the mean winds are carried out in order to identify the accuracy and deviation of the method deriving the background winds and GW variances. A certain number of meteors (from 20 to 300) are randomly selected and the process is repeated by 500 times for each set of simulation. It is found that a larger underestimation of the GW variance exists for a lower meteor rate and when the meteor rate is 20/4hrs, the underestimation is about 10%. The retrieval of the GW variances has a high accuracy and small standard deviation if the meteor rate is larger than 100/4hrs. Although the meteor rate has a diurnal cycle, the diurnal and semidiurnal variations of the GW variances are not related to the meteor rate, but caused by real geophysical mechanisms, possibly by the modulations of the diurnal and semidiurnal tides. The relation between the GW variances, mean winds and tides is discussed and the differences between the three different sites are identified, which can be related to the different dominant tides. In addition, the seasonal variations of the "tidal modulation" on GW variances are compared between the three sites, which are found to be consistent with the seasonal variations of the diurnal and semidiurnal tides. It implies that the GW variances are very likely to be modulated by the mean winds and tidal winds. The derivation based on the meteor radar is capable of providing the horizontal wind variances in a certain spectrum as a proxy of the GW activities. However, the possibility that the time variation of the wave sources may also have impacts on the GW activities is not ruled out for this study, which needs to be evaluated in the future.

MLTG-16 Gravity waves in WACCM with respect to transport of NO_x created by energetic particle precipitation - by Laura Holt

Status of First Author: Student IN poster competition, Undergraduate

Authors: Laura A. Holt, Cora E. Randall, Lynn Harvey

Abstract: In the Arctic winters of 2005-2006 and 2008-2009 we observed that energetic particle precipitation (EPP) can have a significant impact on the middle atmosphere even during times of low geomagnetic activity. Stratospheric EPP-created NO_x (EPP-NO_x) mixing ratios were well above average in both winters, while the level of EPP leading up to the stratospheric NO_x enhancements was low. These increases in stratospheric EPP-NO_x mixing ratios have been attributed to unusually strong descent in the middle atmosphere that transported EPP-NO_x created under normal EPP levels in the mesosphere and lower thermosphere (MLT) to the stratosphere. In order to reproduce the variability of middle atmospheric effects of EPP in general climate models (GCMs)—and thus elucidate the factors controlling the transport of EPP-NO_x from the MLT to the stratosphere—we must be able to reproduce the dynamics that give rise to exceptional descent rates. Since gravity waves are the primary forcing controlling mesospheric descent, it is critical that their parameterization in GCMs be optimally tuned to represent middle atmosphere dynamics. In this study, we assess the gravity wave parameterization in version 4 of the Whole

Atmosphere Community Climate Model (WACCM4) with respect to reproducibility of dynamical features that are relevant to the transport of EPP-NO_x.

MLTG-17 Physical Mechanisms of Gravity Wave Variations and Their Impacts on the MLT during the 2009 Stratospheric Sudden Warming
by Chihoko Yamashita

Status of First Author: Student IN poster competition, PhD

Authors: Chihoko Yamashita (NCAR / University of Colorado), Hanli Liu (NCAR), Xinzhao Chu (University of Colorado)

Abstract: Gravity waves are one of the key elements for driving the atmospheric coupling from the stratosphere to the thermosphere during stratospheric sudden warmings (SSWs). The limited knowledge of gravity wave variations and their source distribution leads to the uncertainty in the SSW simulations. In this study, ECMWF-T799 (~0.25° horizontal resolution and 91 vertical levels up to 0.01 hPa) is used to study gravity wave variations. Gravity wave activities increase around the polar jet prior to the 2009 SSW. The magnitude and occurrence of gravity waves correlate well with the location and strength of the polar vortex that is strongly distorted by planetary wave growth. During the development and onset of SSW, the zonal-mean gravity wave potential energy density (GW-Ep) increases on January 5 and 15-22 in association with the growth of planetary wave wavenumber 1 and wavenumber 2, respectively. The altitude where PWs reach maximum amplitude is initially in the lower mesosphere, and then progress downward. GW-Ep enhancement also seems to show a corresponding descent from January 5-22. GW-Ep peaks before the wind reversal and significantly weakens after the SSW. These variations are confirmed by COSMIC/GPS observations. The physical mechanisms of gravity wave variations and their global impacts on the upper atmosphere will be presented.

Mesosphere and Lower Thermosphere Lidar Studies

MLTL-01 First Results from McMurdo Lidar Campaign - by Xinzhao Chu

Status of First Author: Non-student

Authors: Xinzhao Chu¹, Wentao Huang¹, Weichun Fong¹, Zhibin Yu¹, Zhangjun Wang¹, John A. Smith¹, Cao Chen¹, and Chester S. Gardner²

¹Cooperative Institute for Research in Environmental Sciences & Department of Aerospace Engineering Sciences, University of Colorado at Boulder, USA

²Department of Electrical and Computer Engineering, University of Illinois at Urbana-Champaign, USA

Abstract: Lidar observations of PMC, Fe layers and Fe temperatures at the South Pole (90°S) and at Rothera (67.5°S) have characterized these layers and temperatures at two representative sites. Despite the success of lidar observations at the South Pole and near the edge of Antarctica at Rothera, Davis and Syowa stations (~69°S), a critical data gap existed in latitude between 90°S and 69°S, for PMC by groundbased lidars and for Fe layers by all observational means. Such a data gap hampered the advancement of middle atmosphere research in Antarctica.

Aiming to fill in this critical gap, we deployed an Fe Boltzmann lidar to McMurdo (77.83°S, 166.66°E), half way in between the South Pole and Antarctic Circle, in the austral summer of 2010-2011. This lidar was originally developed at the University of Illinois and deployed to the South Pole (1999-2001) and Rothera (2002-2005) for above observations. It was refurbished and upgraded at the University of Colorado in Boulder from 2009 to 2010 to restore its specifications and incorporate newly available technologies. Through collaborations between the United States Antarctic Program (USAP) and the Antarctic New Zealand (AntNZ), the University of Colorado lidar group installed the Fe lidar into the AntNZ facility at Arrival Heights, McMurdo in November and December 2010.

We report the first lidar observations of polar mesospheric clouds, Fe layers and Fe temperatures at McMurdo, Antarctica in the season of 2010-2011. Through these data we confirm the hemispheric difference in PMC altitude, and reveal a statistically significant latitudinal dependence of PMC altitude, in combination with previous lidar measurements at the South Pole and Rothera. Dramatic variations of meteoric Fe layers and frequent occurrence of sporadic Fe layers are observed and are possibly linked to the high magnetic latitude of McMurdo Station. We also investigate the correlation among MLT temperature, PMC brightness and Fe density, along with the influences by waves.

MLTL-02 Temperature Profiling from McMurdo, Antarctica with a Fe Boltzmann Lidar - by Weichun Fong

Status of First Author: Student IN poster competition, PhD

Authors: Weichun Fong, Xinzhao Chu, Zhibin Yu, Wentao Huang, Zhangjun Wang, Bo Tan

Abstract: An Fe Boltzmann lidar system has been deployed at McMurdo (77.83°S, 166.66°E), Antarctica in the late 2010. Over 500 hours of lidar data have been collected after the accomplishment of the installation in December 2010. The lidar system provides temperature measurement from upper stratosphere to lower mesosphere region by the Rayleigh integration technique. Combining the retrieved temperature from meteoric Fe layer at MLT region, temperature profiles from altitude 30 to 110 km can then be obtained and help to characterize the waves propagation in the atmosphere.

MLTL-03 Wave signatures in Fe temperature measurements over McMurdo by Cao Chen

Status of First Author: Student NOT in poster competition

Authors: Cao Chen, Xinzhao Chu, Weichun Fong, Wentao Huang, Zhibin Yu, Xiaoli Zhang, and Adrian McDonald

Abstract: An upgraded Fe Boltzmann lidar was deployed to McMurdo, Antarctica to measure the thermal structure and composition of middle atmosphere. Apparent wave signatures were observed in several days of iron density and temperature measurements with clear downward phase progression. We will examine the vertical wavelengths and apparent periods of these events. With the help of satellite data (e.g., Aura-MLS and AIM), we will investigate horizontal wave properties and characteristics of these oscillations in order to identify the nature of these waves. Furthermore, we will inspect how these waves affect PMC (Polar mesospheric cloud) and Fe density.

MLTL-04 Simultaneous and Common-Volume Lidar Observations of Mesospheric Na and Fe Layers at Boulder, Colorado (40N, 105W) in 2010 - by Wentao Huang

Status of First Author: Non-student

Authors: Wentao Huang¹, Zhangjun Wang^{1, 2}, Weichun Fong¹, John A. Smith¹, Zhibin Yu¹, Xinzhao Chu¹

¹Cooperative Institute for Research in Environmental Sciences & Department of Aerospace Engineering Sciences, University of Colorado at Boulder, USA

²Ocean Remote Sensing Institute, Ocean University of China, Qingdao, China

Abstract: In summer 2010, we constructed a three-frequency Na Doppler lidar at Boulder, Colorado (40N, 105W). With one telescope pointed vertically, it monitors Na layer and temperature in the mesopause region reliably. At the same time, we were upgrading and calibrating an Fe Boltzmann temperature lidar,

which observed Fe layer and temperature, at the same location before its departure in October to McMurdo, Antarctica. These two lidars have been used to observe the Na and Fe layers in the mesosphere and lower thermosphere (MLT) region from June to September 2010, including many nights of simultaneous and common-volume measurements. We will characterize the observed metal layers of their densities, heights, and widths. More importantly, we will compare and discuss the distinctive features, boundaries and structures, of the simultaneously observed Na and Fe layers. Special nights, for example 11 August 2010 with abnormally high Na and Fe densities, will be examined in details. Although there have been a few reports of simultaneous Na and Fe observations, this is one of the first observations with concurrent temperature measurements. Therefore, these datasets provide a rare opportunity to study chemistry and temperatures of the MLT region.

MLTL-05 Lidar Studies of the Arctic Atmosphere at Chatanika, Alaska - by Richard Collins

Status of First Author: Non-student

Authors: Richard L. Collins, Geophysical Institute, University of Alaska Fairbanks
rlc@gi.alaska.edu

Abstract: This poster presents an update on Rayleigh and resonance lidar studies at the Lidar Research Laboratory (<http://www2.gi.alaska.edu/splidar/>), Poker Flat Research Range, Chatanika, Alaska. Rayleigh lidar studies are focused on (i) the wave-driven wintertime circulation and (ii) noctilucent (or polar) mesospheric clouds in the summertime circulation. Resonance lidar studies are focused on (i) the mesospheric metal layers and (ii) auroral species in the thermosphere. The poster presents current work and future plans (highlighting lidar contributions to multi-instrument, satellite, and rocket-based experiments) at the Geophysical institute of the University of Alaska Fairbanks.

MLTL-06 Mesospheric inversion layers seen by Rayleigh lidar and their relationship to planetary wave structure in the Arctic middle atmosphere - by Brita Irving

Status of First Author: Student IN poster competition, Masters

Authors: Brita K Irving (bkirving@alaska.edu) and Richard L. Collins, Geophysical Institute and Department of Atmospheric Sciences, University of Fairbanks Alaska, Fairbanks, Alaska; Brentha Thurairajah, Bradley Department of Electrical and Computer Engineering, Virginia Polytechnic Institute and State University, Blacksburg, Virginia; Ruth S. Liebermann, Colorado Research Associates, Northwest Research Associates, Boulder, Colorado; Kohei Mizutani, Environmental Sensing and Network Group, National Institute of Information and Communications Technology, Tokyo, Japan.

Abstract: The wintertime circulation of the Arctic middle atmosphere is unstable and variable due to wave-mean flow interactions and forcing by planetary-waves activity. The location of the Rayleigh lidar at Poker Flat Research Range (PFRR), Chatanika, Alaska (65°N, 147°W), provides a unique opportunity to observe the dynamically driven middle atmosphere and study wave-driven forcing of the circulation. This study presents Rayleigh lidar observations at PFRR from November 1997 – March 2009, and characterizes mesospheric inversion layers (MILs) seen in the nighttime temperature profiles. MILs are characterized by a negative lapse rate in the region between the stratopause and mesopause and are considered signatures of vertically propagating planetary waves breaking in this region. High-resolution lidar data is complimented by lower-resolution geopotential height perturbation and temperature data from the Sounding of Atmosphere using Broadband Emission Radiometry (SABER) instrument aboard the TIMED satellite, and are used to study the relationship of MILs and planetary wave activity on a synoptic scale. Our results support the idea that MILs are formed by planetary waves propagating into the middle atmosphere and breaking, as indicated by a westward tilt with height of geopotential height perturbation below the MIL, and coincide with altitudes where planetary wave temperatures undergoes an abrupt phase shift.

MLTL-07 The World's Most Sensitive Rayleigh-Scatter Lidar - by Leda Sox

Status of First Author: Student IN poster competition, PhD

Authors: Vincent B. Wickwar¹, Joshua P. Herron², Marcus J. Bingham¹, Lance W. Petersen¹ (1Physics and CASS, Utah State University, 2Space Dynamics Lab)

Abstract: The Rayleigh lidar system operating since 1993 at the Atmospheric Lidar Observatory (ALO) on the campus of Utah State University (USU) has recently undergone some serious upgrades to both its transmitting and receiving systems. By transmitting two Nd:Yag lasers with average powers of 18 W and 24 W in parallel and by replacing one 44-cm diameter mirror by four mirrors that have a combined area equal to that of a 2.5 m diameter mirror as the receiving telescope we have increased our Power-Aperture Product, or Rayleigh lidar figure of merit, from 2.7 Wm² to 205 Wm². This enhanced sensitivity, along with the addition of two more detector channels, will improve data acquisition and reduction in any of four ways: a greater altitude range (from 45-90 km to 25-110 km), shorter time resolution (from hours to minutes), increased spatial resolution (from 3 km to 37.5 m), or smaller measurement uncertainties. These improvements will help us measure atmospheric phenomena that are at higher altitudes, change more quickly than our original time scale, or are thinner than our original altitude scale. Such phenomena include: upward and downward coupling between regions, sudden stratospheric warmings (and mesospheric coolings), gravity waves and other waves, convective instabilities associated with temperature inversions, noctilucent clouds (NLC) and other thin layers, and summer-winter mesopause transition. Our summer Mesospheric Data Campaign, which will involve a full instrument cluster (e.g., lidars, imagers, cameras, meteor wind radar) at USU and the nearby Bear Lake Observatory, will be centered around the summer solstice on 21 June 2011 in hopes of detecting NLCs, which have been observed near the solstice before and any of the aforementioned phenomena.

MLTL-08 Resonance Fluorescence He LIDAR - by Tony Mangogna

Status of First Author: Student NOT in poster competition

Author: Tony Mangogna

Abstract: The resonance fluorescence He LIDAR is a unique method for measuring temperature and winds in the thermosphere.

MLTL-09 Accounting for nonlinear sensor behavior in laser remote sensing applications - by Robert Andrew Stillwell

Status of First Author: Student IN poster competition, Undergraduate

Authors: Authors: *Robert Stillwell¹, Jeffrey P. Thayer¹, Matthew Hayman²
¹University of Colorado at Boulder, Department of Aerospace Engineering Sciences
²University of Colorado at Boulder, Department of Electrical, Computer and Energy Engineering
*undergraduate student

Abstract: Using the photon counting method to conduct LiDAR measurements presents a fundamental problem when one considers the large dynamic range of signal returns to be processed. As a consequence of the dual requirement for large signal capacities and small signal precision, most LiDAR systems display non-linear behavior where the output count rate measured is not proportional to the incident light intensity observed. This non-linear behavior was found to cause errors in polarization measurements of aerosols and clouds with the ArcLiTe LiDAR system at Sondrestrom, Greenland (67.0o N, 50.9o W) and with the CAPABL LiDAR system at Summit, Greenland (72o N, 38o W) where the extent of saturation was not consistent across measurement channels. In response, a saturation characterization was performed considering the possibility of simultaneous saturation of both the photomultiplier tube (PMT) and discriminator. Using the general LiDAR equation and defining a three channel figure of merit, measured

photon rates were correlated with ideal photon rates to determine the dead times of both PMT and discriminator. This characterization has allowed for the correction of saturated signals which increase the dynamic range of the CAPABL system by an order of magnitude as well as an explanation of consistent depolarization errors with the ArcLiTe system.

Mesosphere or Lower Thermosphere General Studies

MLTS-01 With My Head in the Clouds: Helping to Understand the Boundary Between Earth and Space - by Rachel Jessica Ward

Status of First Author: Student IN poster competition, Undergraduate

Authors: Rachel Jessica Ward

Abstract: At altitudes close to 80 km, there exist icy clouds which glow eerily during the twilight hours and display distinct wave patterns. These are known as Polar Mesospheric Clouds (PMCs). These PMCs are formed by tiny ice particles that scatter blue light (thus, the glow).

In April 2007, the Aeronomy of Ice in the Mesosphere (AIM) satellite was launched into polar orbit to photograph the amazing phenomenon of PMCs. On the AIM satellite is a highly sensitive Cloud Imaging and Particle Size (CIPS) UV imager, which measures the radiance and morphology of PMCs. Since the launch of the AIM satellite, thousands of images of PMCs have been recorded, which are providing key information to understanding the relationship between the temperature, upper mesospheric water chemistry, location, and span of these clouds.

While PMCs have been recorded from the ground for many years, the AIM satellite has some unique advantages which are not shared by its ground-based counterparts. Namely, it can record images at a broader range of latitudes than is possible from the ground, and it allows images to be taken during the summer months of the Northern and Southern hemispheres. Comparison of AIM summer data with previous winter observations will provide further insight to the correlation between gravity waves and PMCs.

MLTS-02 Analysis of the PMC Parameter Retrieval from a CIPS Scattering Profile: High Sensitivity to Uncertainties and Methods Used to Account for this - by Justin Neal Carstens

Status of First Author: Student IN poster competition, PhD

Authors: J N Carstens, S M Bailey, J Lumpe, K Nielsen, C Randall

Abstract: The Cloud Imaging and Particle Size (CIPS) experiment on the Aeronomy of Ice in the Mesosphere (AIM) satellite is a nadir imager with an approximately 2000 km along track by 1000 km cross track field of view. CIPS observes at the UV wavelength of 265nm with a spatial resolution of 1km by 2km. One of the key goals for CIPS is to determine Polar Mesospheric Cloud (PMC) ice particle sizes. The scattering "profile" is the approximately seven albedo measurements obtained by CIPS as AIM passes over each cloud parcel. These are each made at different viewing geometries and thus over a range of scattering angles.

The scattering profile is composed of a Rayleigh background signal and a PMC ice phase function signal. The Rayleigh albedo is controlled by the ozone column density above ~50km as well as the vertical ozone structure in this altitude region. The PMC particle size information is in the PMC phase function. In order to isolate the PMC phase function, we must remove the Rayleigh background albedo. Using an analysis where we decompose the signal into orthogonal components, we will attempt to quantify the degree to which this decomposition is unique. As it turns out, there is a large overlap between the space spanned by

the Rayleigh background and that of the PMC ice phase function signal. This results in a high correlation between background retrieval errors and PMC parameter retrievals. We will address how several types of errors, systematic and random, can propagate into errors in retrieved PMC parameters and how our retrieval algorithms overcome these difficulties.

MLTS-03 AIM/CIPS observation and NOGAPS-ALPHA analysis of polar mesospheric cloud structures - by Brentha Thurairajah

Status of First Author: Non-student

Authors: Brentha Thurairajah, Scott M Bailey, David E Siskind, Cora E Randall, James M Russell III

Abstract: The Cloud Imaging and Particle Size (CIPS) experiment aboard the AIM satellite is a high resolution ultra violet imager that provides images of PMCs from ~40 degree latitude to the terminator. These PMC images from space reveal a variety of structures like bands, billows, and whirls that are also seen in ground based NLC images. An interesting feature not commonly seen in NLC images, but are a ubiquitous feature in the CIPS PMC images is the occurrence of 'ice voids'. Ice voids are nearly circular ice free regions whose diameter varies from <100 - 1000 km. In this study we document the morphology of the larger ice voids as seen in the CIPS images. We investigate the meteorology and dynamics of the environment in which these ice voids form using high-altitude analysis from the NOGAPS-ALPHA forecast assimilation system.

MLTS-04 Solar Energy and Nitric Oxide in the Lower Thermosphere: Observations by the Remote Atmospheric Ionospheric Detection System (RAIDS) and the Solar Dynamic Observatory (SDO) - by Cissi Ying-tsen Lin

Status of First Author: Student IN poster competition, PhD

Authors: C. Y. Lin, J. D. Yonker, S. M. Bailey, K. Minschwaner, S. A. Budzien, A. W. Stephan, T. N. Woods, D. Woodraska, R. L. Bishop, A. B. Christensen, J. H. Hecht

Abstract: Nitric oxide (NO) is a minor constituent of the lower thermosphere which plays numerous key roles there. Its production is very sensitive to those energy sources able to break the strong molecular nitrogen bond; thus NO concentrations are indicative of energy deposition. Cooling through infrared NO emission is a crucial part of the thermospheric energy balance. NO is also the terminal ion in the E-region of the ionosphere. If NO is transported to lower altitudes, it is a catalytic destroyer of ozone. The Remote Atmospheric and Ionospheric Detection System (RAIDS) is a suite of limb viewing radiance monitors observing the lower thermosphere at wavelengths from the EUV through the NIR. An inverse technique is applied to radiance profiles near 237 nm, which contain fluorescence emission on the NO gamma(0,1) band, so that the vertical profile of NO density can be determined. One of the key advantages of RAIDS NO observations compared to previous experiments is that RAIDS is deployed on the International Space Station and thus is able to observe NO concentrations at all sunlit local times. In addition, launched in February of 2010, the EUV Variability Experiment (EVE) on the Solar Dynamic Observatory (SDO) provides solar soft X-ray and EUV measurements with unprecedented spectral resolution (0.1 nm), temporal cadence (10 seconds), and accuracy (20%). We compare the 27-day variation of nitric oxide in the lower thermosphere with the fluctuation of the solar soft X-ray energy. By doing so, we are able to understand better quantify the relationship between solar energy input and NO production and constrain the photochemistry.

**MLTS-05 Simulating Nitric Oxide in the lower Thermosphere using a 3D model
by Karthik Venkataramani**

Status of First Author: Student IN poster competition, Masters

Authors: K.Venkataramani, J.Yonker, S. M. Bailey

Abstract: The NCAR Thermosphere-Ionosphere-Electrodynamics General Circulation Model (TIE-GCM) is a three-dimensional non-linear representation of the coupled thermosphere and ionosphere system. Results from a revised chemistry scheme [Yonker et al, 2011] are introduced into the model and their effects are explored. Specifically, the reaction of atomic oxygen with the first excited electronic state of molecular nitrogen, N₂(A), has been shown to play an important role in the production of NO. Revisions included also lead to an increased production rate of the first excited state of atomic nitrogen, N(2D), whose reaction with O₂ is well known to be the dominant driver for NO production in the lower thermosphere. Preliminary comparisons of NO densities between the modified model and data from the Student Nitric Oxide Explorer (SNOE) have been made, which show a better agreement between the two at high latitudes.

**MLTS-06 The Role of N₂(A) in Production of Lower Thermospheric Nitric
Oxide (NO) - by Justin David Yonker**

Status of First Author: Student IN poster competition, PhD

Authors: Justin D. Yonker, Karthik Venkataramani, Scott M. Bailey, Kenneth R. Minschwaner

Abstract: NO is an important minor species in the upper atmosphere. It cools the thermosphere in response to solar and geomagnetic forcing, is easily ionized to form the principle E-region ion, and is a catalytic destroyer of ionized molecular oxygen and ozone. An essential chemical process driving NO production in the lower thermosphere is the reaction of atomic oxygen, O(3P), with ionized molecular nitrogen, N₂⁺. An important role has recently been ascribed to the reaction of O(3P) with the first excited electronic state of molecular nitrogen, N₂(A). Due to radiative cascade, determination of the N₂(A) production rate is computationally expensive. We show that a simple Gaussian scaling of the photoelectron impact N₂⁺ production rate can recover the N₂(A) production rate to within 10%, enabling it to be efficiently implemented in existing thermospheric models. The modelled N₂(A) is validated by comparison with Vegard-Kaplan spectra from the Ionospheric Spectroscopy and Atmospheric Chemistry (ISAAC) Experiment. Comparison of a 1D photochemical model with the equatorial NO densities from the Student Nitric Oxide Explorer (SNOE) reveals the N₂(A) to be a significant contributor to the NO production rate and improves the comparison between model and data.

**MLTS-07 Tele connection pattern of different altitudes and different
hemispheres derived from SABER and WACCM - by Bo Tan**

Status of First Author: Student IN poster competition, PhD

Authors: Bo Tan, Xinzhao Chu, Hanli Liu, Chihoko Yamashita

Abstract: Temperature observations from Sounding of the Atmosphere using Broadband Emission Radiometry (SABER) are used to study the patterns of tele-connection among different hemispheres and different altitudes. Years with or without Sudden Stratospheric Warming (SSW) are separated and both show qualitatively the same correlation patterns. The tele-connection patterns at all latitudes from 15 to 120 km are reproduced in the Whole Atmosphere Community Climate Model (WACCM). In WACCM, the correlation of residual circulation and temperature are studied and the correlation patterns of vertical residual circulation correspond to temperature correlation patterns. Besides, the inter-annual variations of positive and negative correlation regions in Southern hemisphere are observed in WACCM.

MLTS-08 Investigation of metal and metal ion density profiles in the MLT by satellite remote sensing using data from SCIAMACHY - by Martin Langowski

Status of First Author: Student NOT in poster competition

Authors: Martin Langowski, Christian von Savigny, John Burrows, Miriam Sinnhuber

Abstract: Metals are brought into the upper atmosphere by ablation from meteorites, what leads to a deposition of metal and metal ions in the mesosphere and lower thermosphere. The metals/ions form sharpened peaked layers in the region of 85 km to 110 km. They can be observed by strong airglow emission, due to their big absorption coefficients and oscillation strength. The densities of the metal/ions can therefore be obtained by emission spectroscopy done, e.g., with SCIAMACHY.

SCIAMACHY/Envisat is a grating spectrometer with limb and nadir scan capabilities, launched in 2002. Since mid 2008, additional to the nominal limb scans up to 90 km tangent height, mesosphere-thermosphere scans up to 150 km are performed every two weeks for a day. First results using this data for Mg and Mg⁺ will be presented in this talk.

MLTS-09 Iron Oxide Emission in the Mesosphere - by Deepali Vimal Saran

Status of First Author: Non-student

Authors: D.V. Saran¹, T.G. Slanger¹, W. Feng² and J.M.C. Plane²

¹ Molecular Physics Laboratory, SRI International, Menlo Park, CA 94025

² School of Chemistry, Faculty of Mathematics and Physical Sciences, University of Leeds, UK

Abstract: Emission from the FeO molecule is a long-sought feature in the terrestrial nightglow. Scrutiny of sky spectra from Echelle Spectrograph and Imager (ESI)/Keck II telescope in Mauna Kea, HI, has revealed the presence of a ubiquitous quasi-continuum between 500 and 700 nm, which has been identified as originating with the excited FeO (FeO*) molecule, generated from the reaction between atomic iron and ozone. Comparison with laboratory spectra involving the reaction of Fe and O₃ [West and Broida, 1975, Burgard et al., 2006], as well as meteor trains [Jenniskens et al., 2000], suggest the atmospheric emission is, in fact, due to the emitting states of FeO(5Δ). Integrated areas of the band profile in the 560-620 nm region with ESI show that the overhead continuum intensity is 3-4 times brighter than the sodium 589 nm lines, although the FeO* emission extends well beyond 620 nm, and may reach several hundred Rayleighs. Analysis of the temporal variability of this nightglow feature has revealed that there are interesting nighttime variations that are not reflected in the other two ozone-dependent nightglow emitters, the OH 8-2 band and the Na doublet (589 nm). The temporal behavior of the FeO and OH emissions was compared to model results from the 1-dimensional and time-resolved model FeMOD (iron mesospheric model), which describes the iron chemistry in the mesosphere and lower thermosphere (MLT). The observed and modeled results for nighttime variability from a low latitude site, Mauna Kea (19N, 155W), are presented and their implications for our understanding of the MLT are discussed.

DVS is the recipient of an NSF CEDAR postdoctoral fellowship, NSF grant ATM-0924781. TGS was supported by grant ATM-0637433 from NSF Aeronomy. WF and JMCP are supported by NERC grant NE/G019487/1.

References: Burgard, D. A., Abraham, J., Allen, A., Craft, J., Foley, W., Robinson, J., Wells, B., Xu, C., and D. H. Stedman, (2006), *Appl. Spectrosc.* 60, 99-102.

Jenniskens, P., M. Lacey, B.J. Allan, D.E. Self and J.M.C. Plane, (2000), *Earth, Moon and Planets*, 82-83, 429-434. West, J.B., and H.P. Broida, (1975), *J. Chem. Phys.*, 62, 2566-2574.

MLTS-10 Relaxation of O₂($v = 1$) by Atomic Oxygen and Carbon Dioxide by Deepali Vimal Saran

Status of First Author: Non-student

Authors: Saran, D. V., Pejaković, D. A., Kalogerakis, K. S., Slinger, T. G. and Copeland, R. A.
Molecular Physics Laboratory, SRI International,
333 Ravenswood Ave., Menlo Park CA 94025

Abstract: Water vapor is an important constituent of the middle atmosphere and is key to our understanding of the composition and energy budget in the mesosphere and lower thermosphere (MLT). The Sounding of the Atmosphere Using Broadband Emission Radiometry (SABER) instrument onboard NASA's Thermosphere Ionosphere Mesosphere Energetics and Dynamics (TIMED) satellite retrieves water vapor volume mixing ratios in the 6.3–7.3 μm spectral region. The population of the H₂O(v_2) vibrational level responsible for the above emission is in non-Local Thermodynamic Equilibrium (LTE) above ~ 60 –65 km [López-Puertas et al., 1995]. Recent modeling work [Feofilov et al., 2009] has indicated that the output of the non-LTE model of H₂O emissions is rather sensitive to several reaction rate coefficients that suffer from an inadequate accuracy. Foremost among these reactions are processes involving vibrationally excited oxygen: (1) the vibrational-vibrational (V–V) exchange between the H₂O and O₂($v = 1$) molecules; (2) the vibrational-translational (V-T) relaxation of O₂($v = 1$) by atomic oxygen and, to a lesser extent; (3) the vibrational-vibrational (V-V) exchange between carbon dioxide and O₂($v = 1$) [Feofilov et al., 2009]. The results from laboratory studies at SRI of the collisional removal of O₂($v = 1$) by atomic oxygen at room temperature and temperature relevant to mesopause and polar summer MLT (~ 160 K) are presented here. In addition, measurements of the removal of O₂($v = 1$) by carbon dioxide at room temperature are also presented. Our data analysis employs a more refined approach than our earlier analysis [Pejaković et al., 2004; Saran et al., 2008]. The current analysis is based on a combination of numerical and analytical modeling, which allows for contributions of competing processes to the measured kinetics to be better identified and quantified. This improved data analysis results in a more accurate and tightly constrained value for the rate coefficients. The ongoing efforts at SRI include measurements of the rate coefficient for reaction (1).

This work was supported by the National Aeronautics and Space Administration under grants NNX09AI07G, and NNX09AI12G, and NAG5-13002.

References: Feofilov, A., Kutepov, A. A., García-Comas, M., López-Puertas, M., Marshall, B. T., Gordley, L. L., Manuilova, R. O., Yankovsky, V. A., Pesnell, W. D., Goldberg, R. A., Petelina, S. V., and Russell III, J. M., *Atmos. Chem. Phys.*, 9, 8139–8158, 2009. López-Puertas, M., Zaragoza, G., Kerridge, B.J., and Taylor, F.W., *J. Geophys. Res.*, 100(D5), 9131–9147, 1995. Pejaković, D. A., Campbell, Z., Kalogerakis, K. S., Copeland, R. A., and Slinger, T. G., *Eos. Trans. AGU* 85(47), Fall Meet. Suppl., abstract SA41A-1032, 2004. Saran, D. V.; Pejaković, D. A.; Copeland, R. A. *Eos. Trans.*, AGU 89(53), Fall Meet. Suppl., abstract SA31A-1601, 2008.

MLTS-11 Vibrational Relaxation of OH($v = 7$) with O, O₂, and N₂ - by Jerome Thiebaud, presented by Konstantinos Kalogerakis

Status of First Author: Non-student

Authors: Jerome Thiebaud (1,2), Richard A. Copeland (1), and Konstantinos S. Kalogerakis (1)
(1) Molecular Physics Laboratory, SRI International, Menlo Park, California, USA
(2) Present Address: Thermo Fisher Scientific, Redwood City, California, USA

Abstract: The hydroxyl radical is a key species in the energy budget of the terrestrial atmospheres. In the Earth's upper atmosphere, vibrationally excited OH radicals ($v < 10$) are formed by the H + O₃ reaction. The non-thermal vibrational energy is either emitted as an infrared or visible photon, or converted into translational and internal energy via collisions with ambient gases, particularly O, O₂, and N₂. Accurate

rates for the deactivation of the OH high- v states at mesospheric temperatures are essential in the modeling of both the atmospheric OH emission and the heating efficiency of the H + O₃ reaction. In spite of the central importance of OH energy transfer for understanding the energy balance in the atmosphere, no data exist for the vibrational relaxation of OH($v = 5 - 8$) by O atoms and for the temperature dependence of these processes by O₂.

We have performed laboratory experiments investigating the relaxation of OH($v = 7$) with important atmospheric colliders. To make these measurements, we developed a novel three-laser approach using the following steps:

1. generation of OH($v < 5$) by the O(1D) + H₂ reaction following ozone photolysis at 248 nm by an excimer laser in a mixture containing nitrogen and hydrogen;
2. infrared overtone excitation of the OH($v = 4$) radicals to $v = 7$ at 1.21 micrometers using the pulsed output from an optical parametric oscillator system; and
3. probing the temporal evolution of the OH($v = 7$) population by laser induced fluorescence using the B-X (0,7) band at 213 nm.

Experiments studying OH($v = 7$) relaxation and its temperature dependence will be presented. Our measurements show extremely fast relaxation of OH($v = 7$) by O-atoms. We will discuss the atmospheric implications of these results based on recent modeling calculations.

This work was supported by the NASA Geospace Science Program under Grant NNX08AM47G.

MLTS-12 Finite-difference time-domain modeling of infrasonic waves generated by supersonic auroral arcs - by Victor Pasko

Status of First Author: Non-student

Authors: CSSL, Penn State University, University Park, Pennsylvania, USA
(vpasko@psu.edu)

Abstract: Atmospheric infrasonic waves are acoustic waves with frequencies ranging from ~ 0.02 to ~ 10 Hz [e.g., Blanc, *Ann. Geophys.*, 3, 673, 1985]. The importance of infrasound studies has been emphasized in the past ten years from the Comprehensive Nuclear-Test-Ban Treaty verification perspective [e.g., Le Pichon et al., *JGR*, 114, D08112, 2009]. A proper understanding of infrasound propagation in the atmosphere is required for identification and classification of different infrasonic waves and their sources [Drob et al., *JGR*, 108, D21, 4680, 2003]. In the present work we employ a FDTD model of infrasound propagation in a realistic atmosphere to provide quantitative interpretation of infrasonic waves produced by auroral arcs moving with supersonic speed. We have recently applied similar modeling approaches for studies of infrasonic waves generated from thunderstorms [e.g., Few, *Handbook of Atmospheric Electrodynamics*, H. Volland (ed.), Vol. 2, pp.1-31, CRC Press, 1995], quantitative interpretation of infrasonic signatures from pulsating auroras [Wilson et al., *GRL*, 32, L14810, 2005], and studies of infrasonic waves generated by transient luminous events in the middle atmosphere termed sprites [e.g., Farges, *Lightning: Principles, Instruments and Applications*, H.D. Betz et al. (eds.), Ch.18, Springer, 2009]. The related results have been reported in [Pasko, *JGR*, 114, D08205, 2009], [de Larquier et al., *GRL*, 37, L06804, 2010], and [de Larquier, MS Thesis, Penn State, Aug. 2010], respectively. In the FDTD model, the altitude and frequency dependent attenuation coefficients provided by Sutherland and Bass [*J. Acoust. Soc. Am.*, 115, 1012, 2004] are included in classical equations of acoustics in a gravitationally stratified atmosphere using a decomposition technique recently proposed by de Groot-Hedlin [*J. Acoust. Soc. Am.*, 124, 1430, 2008].

The auroral infrasonic waves (AIW) in the frequency range 0.1-0.01 Hz associated with the supersonic motion of auroral arcs have been extensively studied for over four decades [e.g., Wilson and Nichparenko, *Nature*, 214, 1299, 1967; Wilson, *JGR*, 74, 1813, 1969; *JGR*, 77, 1820, 1972; *JATP*, 37, 973, 1975; *Inframatrics*, (10), 1, 2005]. The Lorentz force and Joule heating are discussed in the existing literature as primary sources producing infrasound waves associated with auroral electrojet [Chimonas and Hines,

Planet. Space Sci., 18, 565, 1970; Chimonas and Peltier, Planet. Space Sci., 18, 599, 1970; Wilson, 1972; Swift, JGR, 78, 8305, 1973; Wilson et al., Planet. Space Sci., 24, 1155, 1976; Chimonas, JATP, 39, 799, 1977; Brekke, JATP, 41, 475, 1979]. We emphasize that up to now no quantitative multi-dimensional modeling of infrasound generation and propagation in a realistic atmosphere in association with supersonic auroras has been conducted. Results indicate, in particular, that a body force $\sim 10^{-8}$ N/m³ acting in the electrojet volume with cross-sectional area 10 km by 10 km is fully sufficient to produce the observed pressure perturbations on the ground ~ 0.2 Pa (2 dynes/cm²) [Wilson, 1969]. We will report quantitative modeling of complex infrasonic waveforms including direct shock and reflected shockwaves, which are refracted back to the earth by the thermosphere [Wilson, 1969].

MLTS-13 Simultaneous observations of meteor echoes with different frequencies (32.55 MHz and 53.5 MHz) - by Kishore Kumar Grandhi

Status of First Author: Non-student

Authors: Kishore Kumar G. and Werner Singer
Leibniz-Institute of Atmospheric Physics

Abstract: The decay time of underdense meteor echoes is an important parameter to estimate the ambipolar diffusion coefficient and hence the temperature in the MLT region. Understanding the processes involved in the meteor decay provides good useful information about the MLT dynamics structure. By using the observations of the meteor radars operated at two different frequencies viz., 32.55 MHz and 53.5 MHz located at Juliusruh (54.6°N, 13.4°E), we tested the frequency dependence of the meteor decay time. According to the theory, at particular altitude the decay time (τ) of the meteor echo is directly proportional to the ratio of square of the radar wavelength λ and ambipolar diffusion coefficient (Da) (i.e., $\tau \propto (\lambda^2 / Da)$). According to the square law, if a meteor has been observed at two frequencies simultaneously at the same height then the ratio of the decay time at two frequencies can be related with the wavelengths as $\tau_1 / \tau_2 = (\lambda_1 / \lambda_2)^n$ and the exponent n is equal to 2. We tested this relation using the simultaneous observations at 32.55 MHz and 53.5 MHz. The two radar systems provide calibrated echo data. We analyse unambiguous detections of underdense meteor echoes with signal-to-noise ratios better than 6 dB and located at zenith angles between 10° and 60°. The later provides reliable height information. The selection of the simultaneous observations is dependent on the time of the observations and position (range, zenith and azimuth) of the meteor. The analysis has been carried out for different Theseasons. The results indicate that the relation square law is not valid for all cases. andS sometimes the decay time is proportional to $\lambda^{3/2}$. exponent n is equal to 1.5. We did the analysis for different seasons and this is true for all most all seasons. The study indicates that some other processes also involving in the meteor decay rather than the ambipolar diffusion. The details will be discussed in the poster.

MLTS-14 Long term behaviour of the MLT quasi-7-day wave at two radar-sites at northern polar latitudes - by Wayne Hocking, presented by Kishore Kumar Grandhi

Status of First Author: Non-student

Author: Wayne Hocking

Abstract: The activity of the mesospheric-lower-thermosphere (MLT) quasi-7-day wave at two northern polar meteor-radar sites is presented. The study is based on long term meteor wind observations over Resolute Bay (75°N, 95°W) (May 1998 to Feb 2009) and Yellowknife (62.5°N, 114.3°W) (June 2002 to Oct 2008). The wave showed clear seasonal variations, with strong activity during winter, more modest occurrence in the equinoxes, and minimum strengths during summer. The period of the quasi-7-day wave was 7.4 ± 0.3 days with little to no systematic seasonal variation in the wave period. The wave was characterized by increasing amplitude with increasing height and with downward phase propagation, suggesting that the wave had its origin at lower heights. The planetary wave (PW) activity was stronger in the zonal component than in the meridional component. The PW activity shows year to year variations, and

appears to be sensitive to the background wind. The possible source mechanisms for the quasi-7-day wave are briefly discussed in the light of current understanding about planetary waves.

MLTS-15 Solar Spectral Irradiance effects on the heating and chemistry of the stratosphere and mesosphere - by Juan Fontenla

Status of First Author: Non-student

Authors: J. Fontenla, LASP-Univ. of Colorado; G. Anderson, AFRL; A. Conley, NCAR

Abstract: We show a study of the modeled Solar Irradiance variations through the UV, visible and IR effects on the heating and chemistry of the stratosphere and mesosphere. The study covers the maximum of the Solar Cycle 23 and quantitatively shows significant effects due to the cycle and in shorter time-scales.

MLTS-16 Long-term Observations of Winds and Waves over Bear Lake Observatory - by Chad Fish

Student NOT in poster competition

Authors: C.S. Fish(1), J. Sojka(2), M. Taylor(2), N. Mitchell(3), F.T. Berkey(4)
1Utah State University - Space Dynamics Laboratory,
2Utah State University - Center for Atmospheric and Space Sciences,
3University of Bath - Centre for Space, Atmospheric & Oceanic Science,
4Utah State University

Abstract: A long-term mesospheric wind data set, spanning the most recent solar cycle, has been acquired at the Utah State University Bear Lake Observatory (BLO) in Garden City, Utah [41.9°N, 111.4°W]. The data set is comprised of imaging Doppler interferometry (IDI) and meteor wind radar (MWR) measurements covering the period of 1998 until present. The IDI measurements were implemented on a NOAA HF Dynasonde radar in 1998 and continued until late 2005. During a 4-month period in 2000, an all-sky VHF SKiYMET MWR operated in conjunction with the Dynasonde and provided a correlative data set between the IDI and MWR wind measurement techniques at BLO. During that brief campaign, IDI wind and tide measurements were found to closely match those measured by the MWR, not only during the day but also at night and at all overlapping heights from 80-95 km. In early 2008, another all-sky VHF SKiYMET MWR was installed at BLO and continues to make wind measurements.

In this paper we present results from the wind, tide, and wave component analysis of this multi-year data set. The analysis includes investigation of the seasonal wind pattern behavior, year to year tidal amplitude and phase characteristics, and planetary wave climatology. The wind measurements are shown to compare well to standard atmospheric model long-term trending predictions, but to also include seasonal and short-term variations that demonstrate a rich variety of mesospheric dynamics at play over BLO.

Mesosphere and Lower Thermosphere Other Tidal or Planetary Waves

MLTT-01 A possible effect of the 2006 Sudden Stratospheric Warming in the lunar semidiurnal tide - by Ana Roberta Paulino

Status of First Author: Student NOT in poster competition

Authors: A. R. Paulino, P. P. Batista, B. R. Clemesha, R. A. Buriti, and N. Schuch

Abstract: Meteor wind data from three Brazilian sites [Sao Joao do Cariri (7.4S; 36.5W), Cachoeira Paulista (22.7S; 45W), and Santa Maria (29.7S; 53.8W)] have been used to study the atmospheric lunar semidiurnal tide in the Mesosphere and Lower Thermosphere (MLT). An unusual amplification of the lunar

tide was simultaneously observed at these stations in January 2006 during a Northern Sudden Stratospheric Warming (SSW) event. The lunar tide reached amplitudes higher than 10 m/s as in the zonal as meridional winds for all stations. Moreover, the zonal wind reversed, and the meridional wind increased during that SSW. These characteristics are likely an evidence of vertical coupling as revealed from the MLT winds.

MLTT-02 Dynamical Response in the Mesosphere and Lower Thermosphere to a Sudden Stratospheric Warming Event in the Southern Hemisphere During 2010 - by Irfan Azeem

Status of First Author: Non-student

Authors: I. Azeem, ASTAR LLC., Boulder, CO.; D. Marsh, Atmospheric Chemistry Division, National Center for Atmospheric Research, Boulder, CO.

Abstract: A sudden stratospheric warming occurred in the Southern Hemisphere (SH) during July-August 2010. This was a minor warming event as the temperature increase in the Southern Hemisphere polar stratosphere was not accompanied by a wind reversal at 10 hPa. Nonetheless the mesosphere and lower thermosphere (MLT) temperature structure was dramatically altered during this event. NCEP Reanalysis is used to chronicle the morphology of the polar vortex in the upper stratosphere leading up to this event. TIMED SABER observations are used to investigate the dynamical response of the MLT region to the 2010 stratospheric warming event in the SH. The results show a highly distorted polar vortex in the upper stratosphere between July 21 and August 14. Thereafter the vortex finally reestablishes itself marking the end of the warming event. SABER observations of the southern polar latitudes during this event show a downward progression of the mesopause accompanied by an increase in the amplitude of the stationary planetary wave (zonal wavenumber 1 component) throughout the MLT region. SABER observations of this event are compared with the predictions of the Whole Atmosphere Community Climate Model (WACCM) numerical model and show good agreement between the two datasets. The WACCM simulation captured all the salient features of the event, viz. changes in the polar night jet, mesopause height, and the polar vortex shape in the upper stratosphere.

MLTT-03 Short-term variability of the $s=1$ nonmigrating semidiurnal tide over the South Pole due to coupling with Northern Hemisphere wave activity - by Frederico Estante

Status of First Author: Student NOT in poster competition

Authors: Frederico Estante

Abstract:

MLTT-04 Quasi-two-day waves in the lower thermosphere - by Jia Yue

Status of First Author: Non-student

Authors: Jia Yue, NCAR, jyue@ucar.edu; Han-Li Liu, NCAR; Loren Chang, University of Colorado

Abstract: The zonal wavenumber 3 planetary wave of period near 2 days (QTDW) is a robust feature in the mesosphere and lower thermosphere (MLT). The QTDW exhibits strong seasonal variability with peaks after summer solstice, revealed by ground-based measurements and satellites. Satellites also found two strong responses of the QTDW in meridional wind, one at summer mid-latitudes near 90 km and the other in the tropical lower thermosphere. This double peak spatial structure of the QTDW observed in late January/early February is simulated by the National Center for atmospheric Research thermosphere-ionosphere-mesosphere-electrodynamics general circulation model (TIME-GCM) with the QTDW prescribed in the lower boundary at 30 km. A series of control runs are performed to study the

characteristics of the QTDW and its corresponding EP flux. By isolating the region of baroclinic instability owing to the summer stratosphere/mesosphere easterly jet from the waveguide ($m^2 > 0$), the strong response at summer midlatitudes is removed while the tropical lower thermosphere one remains. This demonstrates the importance of baroclinic instability on the local amplification of the QTDW. Following Salby's normal mode theory in 1980s, the QTDW response of temperature and horizontal wind in the lower thermosphere well resembles the normal mode structure in a realistic atmosphere. The wave amplitude grows substantially faster than a Lamb wave in a region of large refractive index m , where happens to be in the summer middle atmosphere. The QTDW is then projected onto the normal mode in the lower thermosphere and dissipated by the increasing molecular diffusion and self-generated critical layer. The interaction between the QTDW and migrating diurnal tide is investigated and reveals a direct contribution from the tide to the QTDW amplification. The response of the QTDW in the ionosphere will be briefly discussed.

MLTT-05 Incoherent scatter radar study of the terdiurnal tide in the E- and F-region heights at Arecibo - by Yun Gong

Status of First Author: Student IN poster competition, Masters

Authors: Yun Gong, Qihou Zhou

Abstract: We report the analysis of terdiurnal tide in the meridional wind from 90 to 350 km at a low latitude station. Our data is based on nine days of consecutive observation made by the Arecibo incoherent scatter radar during January 14-23, 2010. The terdiurnal tide is observed to be prominent at E-region heights in the first four days (Jan. 14-18) and at the F-region heights in the last five days (Jan. 18-23). The terdiurnal tide is among the two strongest tidal components in both regions. The vertical wavelength of the terdiurnal tide is about 100 km, and 950 km, for the altitude range of 128 to 142 km, and 180 to 320 km, respectively. The F-region terdiurnal tide amplitude is found to be well correlated with the background wind in the lower F-region. Our analysis indicates that the F-region terdiurnal tide is likely a propagating tide, instead of being generated in-situ via non-linear interactions or thermospheric heating.

MLTT-06 Planetary Wave Disturbances of the Wintertime Polar Upper Stratosphere and Lower Mesosphere: A Summary of Observed Characteristics - by Katelynn Greer

Status of First Author: Student IN poster competition, PhD

Authors: Katelynn Greer, Jeffrey P. Thayer, V. Lynn Harvey

Abstract: The polar wintertime middle atmosphere temperature structure is typically disturbed several times throughout the winter season. The most dramatic type of disturbance is a Sudden Stratospheric Warming (SSW), but there are more frequent disturbances of the upper stratosphere/lower mesosphere (USLM) that impact constituent transport, coupling of atmospheric regions and even the development of SSWs. These disturbances are driven by planetary wave activity that produces regional temperature extrema in the USLM. During each planetary wave event, a baroclinic state is established in the stratosphere; in order to maintain quasi-geostrophic and hydrostatic balances, ageostrophic vertical motion is induced which couples the stratosphere to the mesosphere, producing a 'separated' mesopause and "descended" stratopause. This separated mesopause and strongly disturbed stratopause (temperatures in excess of 50 K above nominal temperatures) are observed in SABER measurements. This behavior is evocative of tropospheric fronts. Previous work has documented and studied individual USLM disturbances in the polar winter. Here, we describe an algorithm to identify USLM disturbances in the 20-year+ record of U.K. Meteorological Office assimilated data. From a compilation of 42 (28) Northern (Southern) hemisphere events, the following characteristics are presented: geographical preference, relative position to the polar vortex, event frequency, development/evolution, and their relationship with SSWs. Finally, inter-hemispheric comparisons show how USLM disturbances exhibit differences in frequency, intensity and thermal structure in the Arctic and the Antarctic.

Sprites

SPRT-01 Sprite Streamer Formation in Under-Voltage Conditions by Burcu Kosar

Status of First Author: Student IN poster competition, PhD

Authors: Burcu Kosar (bkosar@my.fit.edu), Ningyu Liu (nliu@fit.edu), and Hamid K. Rassoul (rassoul@fit.edu)

Abstract: Sprite discharges are large scale natural plasma phenomena occurring due to penetration of quasi-electrostatic lightning field to mesospheric/lower ionospheric altitudes. They consist of filamentary plasma channels known as streamers that are highly non-linear and self-organized ionization waves. It has been generally believed that sprites occur when the lightning field exceeds the conventional breakdown threshold field, E_k , in the lower ionosphere. However, recent analysis of high-speed video observations of sprites and electromagnetic measurements of lightning field found that sprite streamers often appear in the lightning field below the breakdown field with a magnitude range of 0.2-0.8 E_k [Hu et al., JGR, 112, D13115, 2007; Li et al., JGR, 113, D20206, 2008].

In this study, we investigate the possibility of initiation of sprite streamers in under- voltage condition (i.e., lightning field below E_k). It has been speculated that sprite streamers can be initiated from ionospheric ionization patches such as meteor trails or disturbances created by thunderstorm and/or lightning. Here we report our modeling results showing that positive streamers are able to originate from such patches and propagate stably in a uniform ambient electric field below E_k . We compare the streamers from ionization patches to those forming in the vicinity of a conducting sphere in an external field below E_k [Liu et al., JGR, 114, A00E03, 2009] that have been applied to explaining sprite observations.

SPRT-02 Streamer Discharges from Isolated Hydrometeors in Thunderclouds by Samaneh Sadighi

Status of First Author: Student IN poster competition, PhD

Authors: Samaneh Sadighi (ssadighi2009@my.fit.edu), Ningyu Liu (nliu@fit.edu), Joseph Dwyer (jdwyer@fit.edu), and Hamid Rassoul (rassoul@fit.edu)

Abstract: In this study we report modeling work on streamer emission from thundercloud hydrometeors. The lightning initiation hypothesis from the conventional breakdown theory suggests that air electric discharges start with electron avalanches, which lead to the formation of streamers. The developed streamers intensify in thundercloud electric fields and a lightning leader eventually evolves from the stem of the streamers [e.g., Loeb, JGR, 71 (20), 4711, 1966; Phelps, JASTP, 36, 103, 1974; Raizer, Gas Discharge Physics, p. 363, 1991]. So one of the critical components of this theory is to demonstrate that electron avalanches and streamers are able to form and propagate in the field with a magnitude similar to the observed thundercloud electric fields. Many decades of in situ soundings of the thundercloud electric field have failed to provide a sufficient value for the inception of electron avalanches and streamers. To overcome this obstacle, the theory of streamer initiation from thundercloud hydrometeors (water drops, ice crystals, etc.) was brought forward [e.g., Dawson, JGR, 74 (28), 6859, 1969; Griffiths and Latham, Quart. J. Roy. Meteorol. Soc., 100, 163, 1974; Griffiths and Phelps, Quart. J. Roy. Meteorol. Soc., 102, 4019, 1976]. Hydrometeors are abundant in thunderclouds and they can cause significant field enhancement in their vicinity. For this study, a recently developed model of streamer discharges by Liu and Pasko [JGR, 109, A04301, 2004] is utilized and further augmented to investigate whether streamers can successfully originate from isolated hydrometeors in the thundercloud electric field. We report modeling results from our streamer simulations, which show successful formation of streamers from model hydrometeors in a uniform applied electric field below the breakdown threshold.

SPRT-03 Impact of mesospheric ion conductivity variations on the initiation of long-delayed sprites - by Jianqi Qin

Status of First Author: Student NOT in poster competition

Authors: Jianqi Qin, Penn State Univeristy; Sebastien Celestin, Penn State University; Victor Pasko, Penn State Univeristy.

Abstract: Long-delayed sprites are initiated 10 to 100 ms after the onset of causal positive cloud-to-ground lightning events and are believed to be driven by intense continuing currents following the return stroke. In the present work, we investigate the effects of ambient ion conductivity on the dynamics of the electric field produced by continuing currents. It is demonstrated that for the long-delayed sprites the establishment of the streamer initiation region in which electric field exceeds the conventional breakdown field is significantly affected by characteristics of mesospheric ion conductivity profiles.

SPRT-04 Influence of the charge moment change on sprite initiation altitude by Caitano Luiz da Silva

Status of First Author: Student IN poster competition, Masters

Authors: Caitano Luiz da Silva, INPE/Brazil, supercaitano@gmail.com; Fernanda T. São Sabbas, INPE/Brazil, fernandasaosabbas@gmail.com

Abstract: Sprites, together with other Transient Luminous Events, are optical evidences of electrical coupling among the troposphere and upper atmospheric regions. Sprites occur in the form of streamer-like discharges above thunderclouds, triggering physical and chemical processes in the region between 40 and 90 km of altitude. The most accepted sprite onset mechanism involves the penetration of quasi-static electric fields from lightning discharges (usually positive cloud-to-ground flashes) in mesosphere/lower ionosphere, leading to ambient electron heating and ionization of neutral species [Pasko et al., 1997]. When the electric field is high enough to reach the local electrical breakdown threshold, streamers may initiate in the mesosphere and develop into sprites. We construct a numerical model to study the atmospheric response to lightning quasi-electrostatic fields leading to electrical breakdown in the mesosphere. The model is composed of continuity equations for the charged particles coupled with Poisson's equation to evaluate the electric field. We include some of the most relevant physical processes, such as electron impact ionization and field induced attachment. We build up on the previous work of Luque and Ebert [2009] which uses a fluid approach. The positive cloud-to-ground discharge is simulated by the placement of a negative charge at 10 km of altitude through a time-dependent charge transfer function. Here we present an analysis of the effects of realistic shapes for the charge moment change function on the sprite inception mechanism and its relationship with sprite initiation altitude. Modeling results indicate that sprites initiating at lower altitudes are produced by more impulsive lightning discharges, require the removal of more charge (from the thundercloud), and have a shorter delay than sprites produced in higher altitudes.

SPRT-05 Monte Carlo Simulation of Terrestrial Gamma-ray Flashes by Wei Xu

Status of First Author: Student IN poster competition, PhD

Authors: Wei Xu, Sebastien Celestin, Victor P. Pasko

Abstract: Terrestrial Gamma-ray Flashes (TGFs) are high-energy photon bursts originating from Earth's atmosphere. After their discovery in 1994 by the Burst and Transient Source Experiment (BATSE) detector aboard the Compton Gamma-Ray Observatory, this phenomenon has been further observed by the Reuven Ramaty High Energy Solar Spectroscopic Imager (RHESSI), the Fermi Gamma-ray Space Telescope and

the Astro- rivelatore Gamma a Immagini Leggero (AGILE) satellite. Recently, AGILE detected TGFs with energies up to 100 MeV. TGFs are believed to be correlated with lightning processes and typically last for a few milliseconds. They have been identified to be produced through bremsstrahlung radiation of energetic runaway electrons.

We have developed a detailed Monte Carlo model to simulate photon transport in the atmosphere. In this present study, we simulate photons with energies ranging from 10 keV to 10 MeV. Three different types of collisions are taken into account: Photoelectric absorption (main process for energies <30 keV), Compton scattering (main process for energies from 30 keV to 30 MeV) and pair production (main process for energies >30 MeV). The initial photons are generated from energetic electrons produced by lightning during negative corona flashes. We utilize electron energy distribution to define spectral properties of these photons. We simulate the propagation of these photons up to 500 km, which is the typical altitude of satellites detecting TGFs. We will specifically investigate ambient conditions in which TGFs are produced, such as the source altitude and lightning parameters.

SPRT-06 Charge transfer to the ionosphere and to the ground during thunderstorms - by Sotirios A. Mallios

Status of First Author: Student IN poster competition, PhD

Authors: Sotirios A. Mallios, Victor P. Pasko

Abstract: It is accepted that thunderstorms are the main generators in the global electric circuit (GEC) [e. g. Williams, Atmospheric Research, 91, 140, 2009; Mareev, Physics Uspekhi, 53, 504, 2010]. In this current work, we examine the current that is driven to the ionosphere and to the ground before, during and after single negative cloud-to-ground (CG) and intracloud (IC) flashes. A numerical model has been developed, that calculates the quasi-electrostatic fields before the flashes, due to the slow accumulation of the charge in the thundercloud, and after the flashes by taking into account the Maxwellian relaxation of the charges in conducting atmosphere. From these results, the charges that are transferred to the ionosphere and to the ground are calculated. We demonstrate the significance of considering the pre-lightning slow charge accumulation stage, and we use a more realistic profile for modeling the conductivity inside the thundercloud. We define efficiency as the ratio of the total charge transferred to the ionosphere to the net charge neutralized during the IC and GC portions of lightning [Mareev et al., GRL, 35, L15810, 2008] and we show that the efficiency depends mainly on the altitudes of the charges inside the thundercloud and their spatial separation. We show also that the amount of charge that is transferred to the ground is negligible compared to the amount of charge that is transferred to the ionosphere. Finally, we show that typical efficiencies for the pre-lightning phase range between 23-60%, for the negative CG case range between 11-50% and for the IC case range between 20-60% and we compare our results with those published recently by Mareev et al. [GRL, 35, L15810, 2008].

Stratosphere Studies and Below

STRB-01 An analysis of SSW & elevated stratopauses generated in WACCM by Amal Chandran

Status of First Author: Non-student

Authors: Amal Chandran, Richard Collins, Rolando Garcia, Daniel Marsh

Abstract: The Whole Atmosphere Community Climate Model (WACCM) spontaneously generates multiple stratospheric sudden warming (SSW) events in simulations of the period between 1953-2006. These SSWs include extreme warming events where the polar vortex breaks down throughout the stratosphere followed by the reformation of an elevated stratopause at a high altitude, which then gradually

drops in altitude and warms. This is similar to the 2005/2006 major SSW in the northern hemisphere which has been extensively documented and studied from observations. In this study we analyze the general circulation and dynamics of the upper stratosphere and mesosphere during winters with both major and minor warming events as well as during quiet years with no SSW. The SSW is triggered by strong planetary wave activity, which then reverses the polar jet-stream and changes the gravity wave forcing in the middle atmosphere. We also quantify the role of gravity waves in the formation of the elevated stratopause, reformation of the polar vortex, and coupling between the stratosphere, mesosphere, and lower thermosphere. The latitudinal and longitudinal variations in both planetary waves and gravity wave forcing and the relative contributions of each to the circulation during these events are also studied. We present statistics on the frequency of occurrence of SSW events and elevated stratopause events over the 53 winters in the free running version of WACCM and assess the inter-annual variability in the polar circulation.

STRB-02 An Investigation of Gamma Drop Size Distribution aloft using the Chung-Li VHF Radar - by Chao-Hsin Chen

Status of First Author: Student IN poster competition, Undergraduate

Author: Chao-Hsin Chen

Abstract: In this poster, with Chung-Li VHF radar and ground-based 2D disdrometer, we investigate the variation of the drop size distribution (DSD) with the height. The radar-measured precipitation terminal velocity, spectral width and backscattering echo power combined with the DSD from 2D disdrometer are analyzed. The radar data were taken on March 24, 2007, from 22:12 to 24:00, and the disdrometer was continuously operated all the time. The weather type response for the precipitation was a moving front. It has been found that the relation between the slope (Λ) and shape (μ) parameters of the Gamma DSD can be well described by a polynomial of second degree empirically and theoretically. However, it is not clear whether or not the μ - Λ relation of DSD in the air can be described by a second degree polynomial. In this poster, we will show that the estimated slope (Λ) and shape (μ) aloft still follow the relation based on the radar-measured precipitation terminal velocity and the spectral width of raindrop. We also found that the relation between the shape (μ) and the precipitation terminal velocity can be described by an exponential form. The physics behind these relations will be discussed in this poster.

IT - Global Positioning System

IT-GPS-01 Possibilities for Calibrating GPS TEC with ISR Data – by Justin Gyllen

Status of First Author: Student NOT in poster competition

Authors: Justin Gyllen (1), Nils Tolpingrud (2), David Murr (1), and Joshua Semeter (3)

Affiliations:

1) Augsburg College

2) JHU/APL

3) Boston Univ

Abstract: In order to reach ground-based receivers, GPS signals must pass through the ionosphere. This passage delays the propagation of the signals, causing imprecision in GPS receiver location calculations (on the order of 10 meter errors) or the possibility to monitor the total electron content (TEC) along the signal path. Accurate corrections for the propagation delays caused by different paths through the ionosphere require accurate measurements and models of the number of electrons encountered by the GPS signals. Ground-based radars can measure the number of electrons more accurately than GPS devices, but only over a limited region of the ionosphere. We hope to correlate the more accurate ground-based radar data with the more extensive GPS data in order to attribute variations in the latter to the former.

Azeem, Irfan, 22

Bass, Elizabeth, 2

Carstens, Justin, 14

Chandran, Amal, 26

Chen, Cao, 11

Chen, Chao-Hsin, 27

Choe, Jongmin, 2

Chu, Xinzhaoh, 10

Collins, Richard, 12

Criddle, Neal, 8

da Silva, Caitano, 25

Estante, Frederico, 22

Fish, Chad, 21

Fong, Weichun, 11

Fontenla, Juan, 21

George, Richard, 6

Gong, Yun, 23

Grabenhorst, Edward, 5

Grandhi, Kishore Kumar, 20

Greer, Katelynn, 23

Gyllen, Justin, 27

Hocking, Wayne, 20

Holt, Laura, 9

Huang, Wentao, 11

Irving, Brita, 12

Kalogerakis, Konstantinos, 18, 20

Kanwar, Uday, 5

Kim, Jeong-Han, 3

Kosar, Burcu, 27

Langowski, Martin, 17

Lee, Changsup, 7

Li, Zhenhua, 6

Lin, Cissi Ying-tsen, 15

Lu, Xian, 9

Macdonell, Alex, 3

Mallios, Sotirios, 26

Mangogna, Tony, 13

Martin, Thomas, 4

McCubbin, Elizabeth, 4

Nielsen, Kim, 8

Pasko, Victor, 19

Paulino, Ana Roberta, 21

Paulino, Igo, 7

Pugmire, Jonathan, 7

Qin, Jianqi, 25

Sadighi, Samaneh, 24

Saran, Deepali, 17, 18

Smith, Steve, 4

Sox, Leda, 13

Stillwell, Robert, 13

Tan, Bo, 16

Thiebaud, Jerome, 18

Thurairajah, Brentha, 15

Vargas, Fabio, 5

Vaudrin, Cody, 1

Venkataramani, Karthik, 16

Volz, Ryan, 3

Ward, Rachel, 14

Watchorn, Steve, 1

Xu, Wei, 25

Yamashita, Chihoko, 10

Yonker, Justin, 16

Yue, Jia, 22

